The biochemical profile of rat testicular tissue as measured by magic angle spinning ^{1}H NMR spectroscopy

J.L. Griffin[a,*], J. Troke[a], L.A. Walker[b], R.F. Shore[b], J.C. Lindon[a], J.K. Nicholson[a]

[a] *Biological Chemistry, Biomedical Sciences Division, The Sir Alexander Fleming Building, Imperial College of Science, Technology and Medicine, South Kensington SW7 2AZ, UK*

[b] *NERC Centre for Ecology and Hydrology, Monks Wood, Huntingdon, Cambridgeshire PE28 2LS, UK*

Received 5 September 2000; revised 30 October 2000; accepted 30 October 2000

First published online 29 November 2000

Edited by Thomas L. James

Abstract The testis is the principal organ of male fertility, responsible for the production of spermatozoa and their maturation into sperm. However, the underlying biochemistry of the testis is relatively understudied. The fluidic and homogeneous nature of the testis makes it an ideal organ for high resolution magic angle spinning (MAS) ^{1}H NMR spectroscopy. In this study we have catalogued the low molecular weight metabolites. The testis contains large amounts of creatine, of which a substantial proportion was shown to be extracellular using bipolar gradients to measure apparent diffusion coefficients. The tissue also contained relatively high amounts of uridine.

Key words: Magic angle spinning ^{1}H NMR; Testis; Creatine; Diffusion weighted spectroscopy

1. Introduction

High resolution magic angle spinning (HRMAS) ^{1}H NMR spectroscopy is a powerful analytical tool for biological tissues, potentially bridging the divide between ^{1}H NMR spectroscopy of tissue extracts and magnetic resonance spectroscopy (MRS) in vivo [1–4]. The study of tissue using extraction procedures and conventional liquid state NMR is complicated by the need for multiple extraction methods to study both lipophobic and lipophilic phases, and in addition it does not address the composition of cell membrane constituents. Furthermore, it is principally destructive in nature. On the other hand, MRS obtains spectra in vivo, but peak resolution is low mainly caused by the lower fields used by in vivo systems, compounded by chemical shift anisotropy, inter- and intramolecular dipole–dipole coupling and spatially varying bulk magnetic susceptibilities also broadening resonances. This later effect is further compounded by diffusion of molecules through strong susceptibility fields within the tissue. However, by spinning tissue at the magic angle (54.7° to the B_0 field) and at speeds comparable to the dipole–dipole couplings high resolution spectra can be obtained [5], with HRMAS being particularly adept at averaging large local gradient changes. This is especially true for biological tissues where cytosolic metabolites still have a high degree of translational freedom and so modest rotation speeds can be used so that tissue structures are not destroyed [6,7].

Despite its salient role in male fertility, the testis has been relatively understudied in terms of metabolic composition. Here we report the first high resolution MAS ^{1}H NMR spectra from rat testes and catalogue the major metabolites found within this tissue. Furthermore, using diffusion weighted HRMAS ^{1}H NMR spectroscopy of intact tissue, the cellular environment of a number of key metabolites, including creatine, was investigated.

2. Materials and methods

Rats ($n=6$; Sprague Dawley) were maintained on standard laboratory feed (RM1, Special Dietary Services; Witham, UK) prior to killing, and housed in a constant environment room (15.5 h light, 8.5 h dark, 22°C). Animals were killed by cervical dislocation, immediately the testes were excised and 20 mg samples were taken and frozen in liquid nitrogen for HRMAS ^{1}H spectroscopy.

HRMAS ^{1}H NMR spectroscopy was performed at 14.1 Tesla (600 MHz) on a Bruker DRX spectrometer using both a conventional solvent suppression pulse sequence and a Carr–Purcell–Meiboom–Gill spin echo pulse sequence [90-(τ-180-τ)$_n$-acquisition], as a T_2 filter to attenuate the resonances from lipids and large macromolecules [7,8] (typically $n=20$ with a total T_2 filter (2 nt) of 40 ms). Spectral assignments were confirmed by 2-dimensional ^{1}H-^{1}H correlation spectroscopy (COSY) together with values obtained from literature [1–4,6,7]. Samples were spun at 5000 Hz at a constant temperature of 4°C for one-dimensional spectra and at 27°C for two-dimensional spectra (this was for practical reasons as the cooler unit could not be used for overnight acquisitions).

To allow the calculation of apparent diffusion coefficients (ADCs), diffusion weighted spectra were acquired using the bipolar LED pulse sequence with a 100 Gauss/cm (1000 mT m^{-1}) magnetic field gradient applied along the magic angle axis to attenuate metabolite resonances. Diffusion weighted spectra were collected at 27°C. Gradient calibration was confirmed by measuring the ADC of free water ($2.3\pm0.2\times10^{-5}$ cm^2 s^{-1}) in a non-spinning rotor. Spectra were acquired for 32 fractional increments of the gradient field (first gradient = 21 mT m^{-1} with subsequent increments of 31.6 mT m^{-1}) with a 50 ms diffusion period (Δ), gradient pulse length of 1 ms (δ) and a 100 μs gradient recovery time (τ). ADCs were calculated according to the Stejskal–Tanner equation as modified by Wu and colleagues [9]; $\mathrm{Ln}(A_g)=\mathrm{Ln}(A_0)-g^2\gamma^2D(\Delta-\delta/3-\tau/2)$ for a one component system where g is the gradient strength, A_g and A_0 are the resonance height at gradient strength g and during no gradient attenuation, respectively. ADCs were estimated for the slowest diffusing environment for water, creatine and choline resonances using a monoexponential fit for the plot of $\mathrm{Ln}(A_g)$ and (gradient strength)^2 for the final 16 gradient field strength increments. This estimates the attenuation curve as being monoexponential in nature and is valid for multicomponent systems where the ADC to be measured is markedly slower (and so is only effected by the final gradients) than the ADCs of the other environments. Linear least square fits were performed with

*Corresponding author. Fax: (44)-20-7594 3226.
E-mail: j.griffin@ic.ac.uk

0014-5793/00/$20.00
PII: S0014-5793(00)02307-3

$R^2 > 0.95$ taken as the limit whereby the attenuation of the final gradients could be modelled using a one component system. For water the attenuation curve was also modelled to a biexponential and a triexponential fit to investigate the possible effects of metabolic compartmentation. This approach was compared with subtracting a monoexponential fit to the final data points and subtracting this contribution from the signal attenuation and then refitting the remaining signal attenuation to another exponential. To justify the level of exponential fit, the least number of components was used with $R^2 > 0.95$ for a plot of $\mathrm{Ln}(A_g)$ and (gradient strength)^2 for each individual component.

Results are presented as means ± standard error of the mean.

3. Results

Spectra obtained from testicular tissue were of comparable resolution to those obtained using conventional liquid state NMR of extracts. Line widths of low molecular weight molecules were ~1 Hz in line width for both conventional solvent presaturation and CPMG pulse sequences (Fig. 1). Testicular tissue had high concentrations of lactate, alanine and in particular creatine and phosphatidylcholine. To assist in assignment of ^{1}H NMR resonances, COSY spectra were also acquired (Fig. 2; Table 1).

The high concentration of creatine was particularly intriguing as the metabolite is also found in high concentrations in seminal fluid. To examine the cellular environment of creatine, a series of diffusion weighted spectra was acquired. A linear fit was applied to the natural log of signal intensity against increasing gradient strength squared for water, creatine and choline for the final 16 gradient increments. While both water and choline had low ADCs consistent with an intracellular environment the ADC for creatine was comparable with that of free water (ADCs/$\times 10^{-6}$ cm^2 s^{-1}: water = 5.8 ± 1.4; choline = 4.7 ± 1.1; creatine = 14.1 ± 3.4; free water 23 ± 0.2).

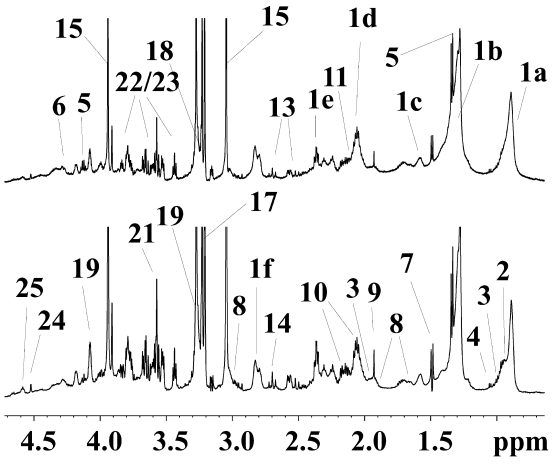

Fig. 1. High resolution MAS ^{1}H NMR spectra of ~10 mg of rat testicular tissue. One-dimensional spectra were acquired using both a conventional solvent presaturation pulse sequence (Upper panel) and a CPMG T_2 weighted pulse sequence (Lower panel) to attenuate macromolecular resonances. For both pulse sequences resolution was comparable with that of conventional liquid state NMR with metabolite line widths of ~1 Hz. See Table 1 for key to figure.

Examining the attenuation of the water resonance, and subtracting successive monoexponential fits from the curve three

Table 1
List of metabolites identified in one- and two-dimensional ^{1}H spectra

Metabolite	Resonance	Key to figures
Lipid triglycerides	0.93 (a) CH_3, 1.30 (b) CH_2, 1.57 (c) CH_2CH_2CO, 1.69 (d) $CH_2CH_2C=C$, 2.0 (e) $CH_2C=C$, 2.8 (f) $=CH–CH_2–CH=$, 5.20 (g) $=CH$	1
Leucine	0.95 d, 0.97 d, 1.71 m	2
Isoleucine	0.93 t, 1.00 d, 1.96 m	3
Valine	0.97 d, 1.02 d, 2.24 m	4
Lactate	1.33 d, 4.10 q	5
Threonine	1.32 d, 4.24 m	6
Alanine	1.44 d, 3.76 q	7
Lysine	1.69 m, 1.91 m, 2.9, 2.96	8
Acetate	1.92 s	9
Glutamine	2.08 m, 2.41 m	10
Glutamate	2.14 m, 2.36 m	11
Aspartate	2.63 dd, 2.81 dd	12
Citrate	2.52 d, 2.62 d	13
Sarcosine	2.54	14
Creatine	3.04 s, 3.93 s	15
Taurine	3.26 t, 3.46 t	16
Choline	3.20 s	17
Phosphocholine	3.24 s	18
Phosphatidylcholine	3.28 s	19
Phosphoethanolamine	3.15, 3.85	20
Glycine	3.61 s	21
Glucose	3.40 t, 3.42 t, 3.47 ddd, 3.54 dd, 3.71 t, 3.76 m, 3.84 m, 4.64 d, 5.23 d	22
Myo-inositol	3.28 t, 3.56 dd, 3.63 dd, 4.06 t	23
N-methyl nicotinate	4.52 s	24
Glutathione	4.58 m	25
Tyrosine	6.87 d, 7.17 d	26
Uridine	4.32 m, 5.82 d, 5.87 d, 7.90 d	27
Artifacts (N-type COSY peaks)		28
CH–NH peptide linkages	3.83, 3.91, 4.22, 8.10, 8.23	29
Methionine	2.14 s, 2.16 m	30
N-acetyl	2.16 s	31

The resonances used to identify the metabolites are listed along with resonance multiplicities (s, singlet; d, doublet; t, triplet; m, multiplet). Numbers refer to key used in figures. Resonances listed in ppm.

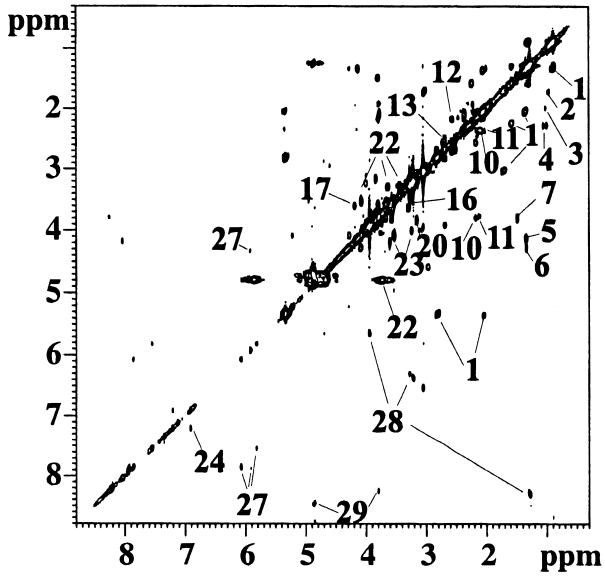

Fig. 2. Metabolite assignments were confirmed using COSY ^{1}H-^{1}H experiments. A number of low molecular weight metabolites were clearly visible as well as cross correlations from lipids (1). See Table 1 for key to figure.

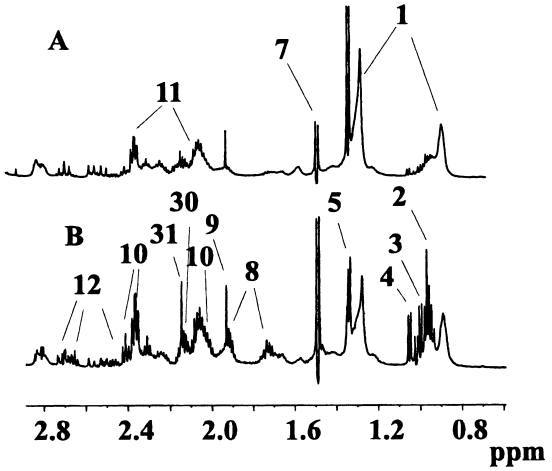

Fig. 4. Degradation of tissue induced by time (~14 h) and spinning at 6000 Hz. A: CPMG spectrum immediately acquired. B: CPMG acquired after 14 h of spinning at 27°C. The CH_3 alanine resonance (7) increased in intensity while that of CH_3 lactate decreased indicative of prolonged anoxia within the tissue. Degradation caused increases in resonance intensities for a number of amino acids including leucine (2), isoleucine (3), valine (4), glutamate and glutamine (10, 11) as well as acetate (8). Prolonged spinning also reduced the intensity of the CH_2 lipid resonance (1). For key see Table 1.

distinct water environments described the shape of the curve (ADCs/$\times 10^{-6}$ cm^2 s^{-1}: 82 ± 9, 16.2 ± 4.1 and 4.9 ± 0.6). Applying bi- and triexponential curve fits to the attenuation, a three component model fitted the data best. A biexponential fit was also used to fit the attenuation of the H_2O resonance in a spinning rotor containing water and D_2O only (ADCs/$\times 10^{-6}$ cm^2 s^{-1}: 158 and 20.2).

To examine further the cellular environment, the one-dimensional NMR spectra that contribute to the pseudo-two-dimensional spectrum were examined. At the maximum gradient strength, the intensities of the phosphatidylcholine singlet ($\delta = 3.28$) and lipid resonances at $\delta = 0.93$ and 1.30 were comparable suggesting that the majority of testicular lipid was in the form of phosphatidylcholine (Fig. 3). No triglyceride backbone resonances were detected at high gradient field strength further confirming this assignment.

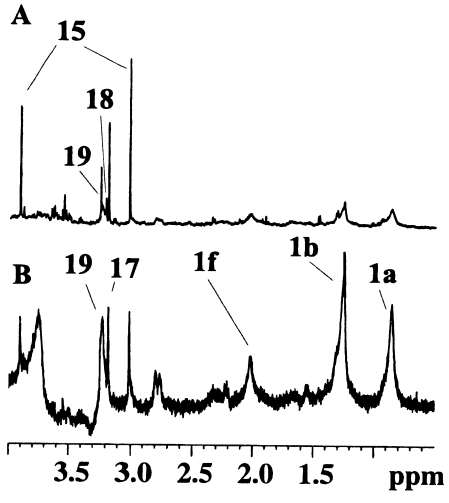

Fig. 3. One-dimensional spectra from the pseudo-two-dimensional diffusion weighted spectra used to obtain diffusion coefficients. The gradient strength was increased from 5% (A) to 100% (B) during the experiment. Spectra are not to scale and relative peak heights should be judged assuming noise levels are constant. For key see Table 1.

To assess the dual effects of spinning rate and tissue degradation with time on testicular tissue, one-dimensional spectra were acquired after the COSY spectra. After 14 h of spinning, the resonances of the glycolytic products lactate and alanine were increased as were those associated with non-polar amino acids in the $\delta = 0.90$–1.10 region of the spectra (Fig. 4). The CH_2 ($\delta = 0.93$) lipid resonance decreased in intensity with respect to both the amino acids and the CH_3 ($\delta = 1.30$) lipid resonance.

4. Discussion

The testis is an 'ideal' organ for study by HRMAS ^{1}H NMR spectroscopy as the tissue has little interfering connective tissue. The organ largely consists of seminiferous tubules with four main different cell types. Loops of seminiferous tubules occur in close proximity to Sertoli cells, where germ cells mature into spermatozoa. There are also interstitial cells of Leydig, responsible for producing and secreting androgenic steroids. This loose collection of cells ensures that B_0 effects are limited to across the cell rather than across the tissue as a whole. This, combined with the improvements caused by HRMAS ^{1}H NMR, produced spectra of a resolution comparable to tissue extracts.

Creatine dominated the spectra obtained. Sperm cells are unusual in that they appear to require large extracellular concentrations of creatine to maintain cell viability and function. Lee and co-workers [10] observed in seminal vesicles a concentration of creatine 65 and 100 times more concentrated than in the blood plasma of the mouse and rat, respectively, and stated that testicular sperm cells are exposed to the highest concentration of creatine in any mammalian tissue. Furthermore, using ^{31}P NMR, they demonstrated that a quarter of the extracellular creatine was phosphorylated in seminal

vesicle fluid [10], finding no evidence that the creatine was from lysed cells and instead suggesting that phosphocreatine was actively secreted for sperm metabolism.

Our HRMAS ^{1}H NMR spectroscopy study agrees with these findings, with developing spermatozoa exposed to a large pool of extracellular creatine, accounting for the majority of the creatine detected using ^{1}H NMR spectroscopy. Using a 'magic angle' gradient, we estimated the ADCs for the slowest diffusing pools of choline, creatine and water. While choline possessed an ADC comparable to that found for intracellular water, the ADC for creatine was greatly in excess of these values, indicating the signal attenuations across the last (strongest) 16 gradients were from intracellular choline, but extracellular creatine. This does not preclude intracellular creatine/phosphocreatine within testicular cells, although it does indicate that this creatine pool would have low NMR visibility. This demonstrates the versatility of ADC measurements using a high resolution MAS probe, as the molecular environment in intact tissue for relatively low concentration metabolites can be probed, just as in cell cultures [11–13] and red blood cell suspensions [14–16]. Modelling changes in ADCs using such a high resolution system may also aid the interpretation of magnetic resonance images as diffusion is commonly used as a means of contrast.

Examination of the attenuation curves of water suggested that there are three environments detected during MAS ^{1}H NMR spectroscopy. Ignoring exchange of water, the data were best fitted to three exponentials which appear to be caused by intra- and extracellular water along with a third pool with an ADC four-fold faster than free water. In a spinning rotor containing only water and D_2O a proportion of water also possessed an ADC greater than that of free water. While subtle rotor fluctuations in spin speed can cause an artificial term that appears diffusive in nature, our ADC measurements were made along the magic angle axis and should not be effected by fluctuations. We suggest this artifactual term arises from convective heating within the rotor (a proportion of which will be resolved along the magic angle axis). For the gradient strengths used this most effected the first five gradients and these were ignored in calculations of ADCs. To simplify calculations the effects of varying susceptibility fields within the tissue (expected to be small across tissues) and exchange of metabolites across the cell membrane (largely restricted to specific transporters in this example) were ignored, both expected to modify the true ADC values [12]. However, our simplified ADC calculations can be used to probe the environment of metabolites using diffusion weighted spectra.

The high resolution spectra that were obtained using HRMAS ^{1}H NMR are ideal for assessing the metabolic status of the tissue. The CH_3 resonance of lactate was readily observable and not obscured by the CH_2CH_2 resonance of lipid triglycerides, as occurs in MAS ^{1}H spectra of more fatty tissue [2,7,11,13]. This is particularly relevant to a number of disorders that result in atrophy of the testes as this is usually induced by a reduction in blood flow into the tissue. For example, chronic alcoholism can induce testicular atrophy and is also known to reduce Leydig cells production of testosterone [17], possibly by altering the NAD/NADH ratio via testicular alcohol dehydrogenase. By measuring the ratio of alanine to lactate one can infer changes in the cytosolic redox potential with alanine rising during severe hypoxia in cerebral tissue [18]. Following the acquisition of 2D data sets the ratio of lactate to alanine decreased suggesting that as in the brain, this ratio may be a good indicator of hypoxia/ischemia. Furthermore, Sertoli cells are known to export lactate specifically for pachytene spermatocyte and spermatid metabolism, and so the concentration of testicular lactate may be highly indicative of sperm cell viability [19].

Hypo-taurine has been detected in goat epididymis and is thought to be an important compound in maintaining sperm viability by acting as an anti-oxidant [20]. However, no hypotaurine was detected in the testes. Instead, taurine, the oxidation product, was detected alongside glutathione, suggesting that in the testes glutathione is the prevalent anti-oxidant. Patel and co-workers [20] have also suggested that myo-inositol may be important for sperm cell maturation, as in the epididymis the concentration of myo-inositol decreases while that of scyllo-inositol increases across the structure as the sperms mature. Only myo-inositol was detected in the testes in this study.

Uridine was also detected in the testicular tissue and is known to be found in high concentration in human seminal fluid [21]. However, seminal fluid uridine is thought to originate from seminal vesicles as UMP, being rapidly converted to uridine at ejaculation by prostatic phosphatase activity [21]. Intracellular uridine kinase activity decreases during sperm cell development, suggesting that activity is related to cellular RNA synthesis [22]. Thus, the detection of a relatively large concentration of this pyrimidine both in the testes and in seminal fluid is indicative of a rapidly dividing cellular environment, as is known to occur in the testes.

Unsurprisingly, a number of degradation products were detected in testicular tissue left at room temperature for over 12 h. The mechanical damage caused by prolonged spinning may have improved the visibility of a number of other amino acids as well. However, the reduction in the CH_2 lipid resonance at $\delta = 1.30$ is curious. Fats are only oxidatively metabolized and any mechanical damage to lipid pools would have made the fats more soluble and hence increased their 'NMR visibility' rather than cause the decrease detected. A number of enzymes are known to be secreted by the prostate gland and seminal vesicles to modify the fluidity of ejaculated semen in a time dependent manner [21]. It is possible that some of the changes detected may be caused by peptidases secreted within the testes and this warrants further investigation.

In conclusion, HRMAS ^{1}H NMR spectroscopy is an ideal technique to study soft tissue organs such as the testis. Spectra obtained are of a resolution comparable to conventional liquid state NMR, but the technique has the advantage of observing lipid soluble and cell membrane metabolites. This is particularly relevant for investigations into testicular cancer where cell proliferation results in cell membrane turnover and a resultant rise in lipophilic compounds such as phosphatidylcholine. Furthermore, using gradients one can investigate directly the microenvironments that a metabolite exists as exemplified by creatine in the testes.

Acknowledgements: This work was supported by a Natural Environment Research Council, UK, Environment Diagnostic Grant. J.L.G. is a Royal Society University Research Fellow.

References

[1] Cheng, L.L., Lean, C., Bogdanova, A., Wright, S., Ackerman, J.,

Brady, T. and Garrido, L. (1996) Magn. Reson. Med. 36, 653–658.
[2] Millis, K., Maas, W., Cory, D. and Singer, S. (1997) Magn. Reson. Med. 38, 399–403.
[3] Moka, D., Vorreuther, R., Schicha, H., Spraul, M., Humpfer, E., Lipinski, M., Foxall, P.J.D., Nicholson, J.K. and Lindon, J.C. (1997) Anal. Comm. 34, 107–109.
[4] Cheng, L.L., Ma, M.J., Becerra, L., Hale, T., Tracey, I., Lackner, A. and Gonzalez, R.G. (1997) Proc. Natl. Acad. Sci. USA 94, 6408–6413.
[5] Andrew, E.R. and Eades, R.G. (1959) Nature 183, 1802.
[6] Tomlins, A., Foxall, P.J.D., Lindon, J.C., Lynch, M.J., Spraul, M., Everett, J. and Nicholson, J.K. (1998) Anal. Comm. 35, 113–115.
[7] Garrod, S., Humpfer, E., Spraul, M., Connor, S.C., Polley, S., Connelly, J., Lindon, J.C., Nicholson, J.K. and Holmes, E. (1999) Magn. Reson. Med. 41, 1108–1118.
[8] Meiboom, S. and Gill, D. (1958) Rev. Sci. Instrum. 29, 688.
[9] Wu, D., Chen, A. and Johnson, C.S. (1995) J. Magn. Reson. (Ser. A) 115, 260–264.
[10] Lee, H.J., Fillers, W.S. and Iyengar, M.R. (1988) Proc. Natl. Acad. Sci. USA 85, 7265–7269.
[11] Millis, K., Weybright, P., Campbell, N., Fletcher, J.A., Fletcher, C.D., Cory, D.G. and Singer, S. (1999) Magn. Reson. Med. 41, 257–267.
[12] Pfeuffer, J., Flogel, U., Dreher, W. and Leibfritz, D. (1998) NMR Biomed. 11, 19–31.
[13] Weybright, P., Millis, K., Campbell, N., Cory, D.G. and Singer, S. (1998) Magn. Reson. Med. 38, 337–344.
[14] Garcia-Perez, A.I., Lopez-Beltran, E.A., Kluner, P., Luque, J., Ballesteros, P. and Cerdan, S. (1999) Arch. Biochem. Biophys. 362, 329–338.
[15] Torres, A.M., Michniewicz, R.J., Chapman, B.E., Young, G.A.R. and Kuchel, P.W. (1998) Magn. Reson. Imag. 16, 423–434.
[16] Stanisz, G.J., Li, J.G., Wright, G.A. and Henkelman, R.M. (1998) Magn. Reson. Med. 39, 223–233.
[17] Ellinghoe, J. and Varanelli, C.C. (1979) Res. Commun. Chem. Pathol. Pharmacol. 24, 87–102.
[18] Griffin, J.L., Rae, C., Dixon, R.M., Radda, G.K. and Matthews, P.M. (1998) J. Neurochem. 71, 2477–2486.
[19] Jutte, N.H., Jansen, R., Grootegoed, J.A., Rommerts, F.F., Claussen, O.P. and van der Molen, H.J. (1982) J. Reprod. Fertil. 65, 431–438.
[20] Patel, A.B., Srivastava, S., Phadke, R.S. and Govil, G. (1999) Anal. Biochem. 266, 205–215.
[21] Tomlins, A.M., Foxall, P.J.D., Lynch, M.J., Parkinson, J., Everett, J.R. and Nicholson, J.K. (1998) Biochim. Biophys. Acta 1379, 367–380.
[22] Haugen, T.B., Hansson, V. and Fritzson, P. (1988) J. Reprod. Fertil. 83, 655–661.